Hindawi Publishing Corporation
International Journal of Photoenergy
Volume 2014, Article ID 739096, 7 pages
http://dx.doi.org/10.1155/2014/739096

Research Article

Effect of Different Deposition Power of In_2O_3 Target on the Characteristics of IGZO Thin Films Using the Cosputtering Method

Shang-Chao Hung,[1] Kin-Tak Lam,[2] Cheng-Fu Yang,[3] and Yu-Jhen Liou[3]

[1] *Department of Information Technology and Communication, Shih Chien University, Kaohsiung Campus, Kaohsiung 84550, Taiwan*
[2] *Institute of Creative Industries Research, Xiamen Academy of Arts and Design, Fuzhou University, Xiamen 361021, China*
[3] *Department of Chemical and Materials Engineering, National University of Kaohsiung, Kaohsiung 81148, Taiwan*

Correspondence should be addressed to Cheng-Fu Yang; cfyang@nuk.edu.tw

Received 1 June 2014; Revised 24 June 2014; Accepted 14 July 2014; Published 10 August 2014

Academic Editor: Giuseppe Carbone

The (In, Ga, Zn)O_x (IGZO) thin films were deposited on glass substrates using cosputtering method in radio frequency magnetron sputtering system. $Zn_2Ga_2O_5$ (Ga_2O_3-2 ZnO, GZO) and In_2O_3 ceramics were used as targets and dual guns were used to deposit the IGZO thin films. Deposition power of GZO target was 80 W and deposition power of pure In_2O_3 target was changed from 70 W to 100 W, and the deposition time was 30 min. The effect of deposition power of In_2O_3 target on the crystalline, surface, electrical, and optical properties of the IGZO thin films was investigated at room temperature in a pure Ar atmosphere. The cosputtered IGZO thin films showed a very smooth and featureless surface and an amorphous structure regardless of the deposition power of In_2O_3 target due to the room temperature sputtering process. However, the cosputtered IGZO thin films exhibited transparent electrode properties because they had high transmittance ratio and low resistivity. The value variations in the optical band gap (E_g) values of the IGZO thin film were evaluated from the plots of $(\alpha h\nu)^2 = c(h\nu - E_g)$. We would also show that the deposition power of In_2O_3 target would have a large effect on mobility and E_g value of the IGZO thin films.

1. Introduction

The hydrogenated amorphous silicon (α-Si:H) thin-film transistor (TFT) has been the work material in the active-matrix liquid-crystal display (AM-LCD) industry for a long time. The typical plasma enhanced chemical vapor deposition (PECVD) α-Si:H TFT has field effect mobility (μ_{eff}) of 0.6~0.8 cm^2/Vs, subthreshold swing of 0.3~0.4 V/decade, off-state drain current (I_{Doff}) below 10^{-13} A, and on-to-off ratio about 10^7 [1]. The α-Si:H TFT backplane configuration does not work well in such short time and the pulse/clock signal can be distorted [2]. To address this issue, proposed solutions are focused on reducing the gate bus-line RC propagation delay, such as adding gate planarization layer [3], adopting buried bus-line structure [4], or using low resistance Cu interconnection [5]. The other emerging area in AM-flat panel display (FPD) is the emissive display such as active-matrix organic light-emitting display (AM-OLED), where the organic light-emitting diode (OLED) is directly integrated with the TFT pixel electrode circuit. AM-OLED avoids the need of backlight and its dynamic range of brightness can be controlled at the pixel level, which is ideal for TV applications [6]. However, conventional metal oxide semiconductors (TCOs) such as zinc oxide (ZnO) are polycrystalline in nature, even at room temperature. The grain boundaries of such metal oxides could affect device properties, such as uniformity and stability, over large areas. Recently, transparent amorphous oxide semiconductors (TAOSs) thin films, such as Sn-Zn-O (SZO), In-Zn-O (IZO), and In-Ga-Zn-O (IGZO), have received a considerable attention in the large-area FPD industry since they may overcome the difficulties encountered in the amorphous α-Si:H and polycrystalline

silicon TFTs (poly-Si TFT) technologies [7]. For that, over the last several years, there has been great interest in thin-film transistors made of TAOSs.

This is mainly due to TAOSs thin-film transistors having unique advantages, such as visible light transparency, large-area uniform deposition at low temperature, and high carrier mobility. The α-IGZO thin films were deposited on polyethylene terephthalate at room temperature and exhibited Hall effect mobility exceeding 10 $cm^2 V^{-1} s^{-1}$, which is an order of magnitude larger than for hydrogenated amorphous silicon [8]. IGZO thin films are a semiconducting material and they can be used as the TFT backplane of FPDs. IGZO-TFT was developed by Professor Hosono's group at Tokyo Institute of Technology and Japan Science and Technology Agency (JST) in 2003 for crystalline IGZO-TFT [7] and in 2004 for amorphous IGZO-TFT [8]. IGZO-TFT has 20–50 times higher mobility than that of amorphous silicon, which has been used for current liquid-crystal displays (LCDs) and electronic papers. Therefore, the IGZO-TFT can improve operation speed, resolution, and size of FDPs, and it is also considered as one of the most promising TFTs to drive OLED displays. In the past, various techniques, such as electron beam evaporation, ion beam assisted deposition, and ion implantation, were used for growth of the IGZO thin films. For example, Nomura et al. got the IGZO thin films by codepositing the Ga:In_2O_3 and Zn:In_2O_3 targets to deposit the Ga and Zn codoped In_2O_3 electrode at room temperature [8]. In the past, Ohta et al. used the high-resolution transmission electron microscopy (HR-TEM) to analyze the IGZO thin films and they found that the HR-TEM image of *sc*-IGZO thin film clearly shows a layered structure [9]. Nomura et al. presented that IGZO crystal is composed of alternating stacks of InO_2^- and $GaO(ZnO)^+$ layers and the In_2O_3 concentration has large effect of the characteristics of the IGZO thin films, especially in the electrical properties [10]. In this study, we first prepared $Zn_2Ga_2O_5$ and In_2O_3 targets separately and cosputtering method was used to deposit the IGZO thin films at room temperature on glass substrates. This study examined the structural, surface, optical, and electrical properties of the IGZO thin films as a function of deposition power of In_2O_3 target.

2. Experimental

Ga_2O_3 powder (99.99%) was mixed with ZnO powder (99.99%) to form the Ga_2O_3-2 ZnO composition (abbreviated as GZO). After being dried and ground, the GZO powder was calcined at 800°C for 1 h and then ground again. GZO powder and pure In_2O_3 powder were mixed with polyvinyl alcohol (PVA) as binder. The mixed powders were uniaxially pressed into pellets of 5 mm thickness and 54 mm diameter using a steel die. After being debindered, the GZO and pure In_2O_3 pellets were sintered at 1200°C and 1250°C, respectively, for 2 h. Glass substrates (Corning 1737) with an area of 2 × 2 cm^2 were cleaned ultrasonically with isopropyl alcohol (IPA) and deionized (DI) water and then dried under a blown nitrogen gas. Then, GZO and pure In_2O_3 targets were used to deposit the thin films at the same time. Deposition power of GZO was 80 W and deposition power of pure In_2O_3 was changed from 70 W to 100 W, respectively; room temperature (RT) was used as deposition temperature, and deposition time was 30 min. The base pressure of sputtering chamber was below 5×10^{-6} Torr and the working pressure was maintained at 3×10^{-3} Torr in pure Ar (99.99%) ambient. Thickness and surface morphology of the IGZO thin films were measured using a field emission scanning electron microscopy (FESEM), and their roughness and crystalline structures were measured using atomic force microscopy (AFM) and X-ray diffraction (XRD) patterns with Cu Kα radiation (λ = 1.5418 Å). Energy dispersive spectrometer (EDS) and secondary ion mass spectrometry (SIMS) analyses were used to find the variation in the concentration of the IGZO thin films. The optical transmission spectrum was recorded using a Hitachi U-3300 UV-Vis spectrophotometer in the 250–1000 nm wavelength range, while the Hall effect coefficient of the IGZO thin films was measured using a Bio-Rad Hall setup.

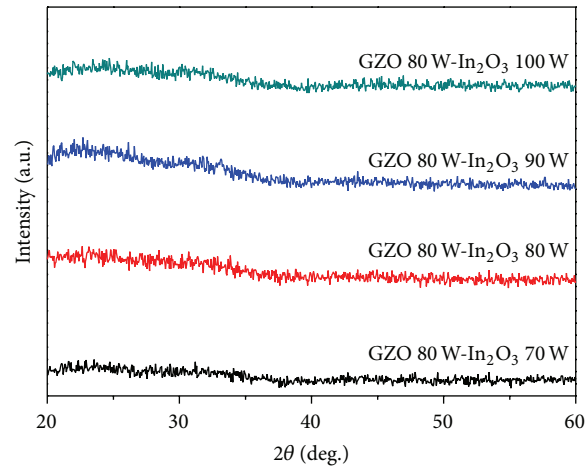

Figure 1: XRD patterns of IGZO thin films as a function of deposition power of In_2O_3 target.

3. Results and Discussion

As the different sintering temperatures are used, the differently crystalline phases will be formed in the IGZO ceramic targets, and the multicrystal phases are only observed in the IGZO ceramic targets. Lo and Hsieh found cubic Ga_2ZnO_4 spinel and rhombohedral $InGaZnO_4$ phases are identified in the 1100°C-sintered sample in addition to the as-prepared oxide powder phases of In_2O_3, Ga_2O_3, and ZnO [11]. However, most of the IGZO thin films will reveal the amorphous phase rather than the polycrystal phases. For example, Jeong and Kim codeposited the Ga:In_2O_3 and Zn:In_2O_3 targets to obtain the IGZO thin films, which revealed the amorphous phase [12]. Jung et al. deposited the IGZO thin films by using the facing targets sputtering (FTS) method at room temperature; also only the amorphous phase was observed [13]. The diffraction intensity of $InGaZnO_4$ phase was not observed in XRD patters, as Figure 1 shows. The cubic

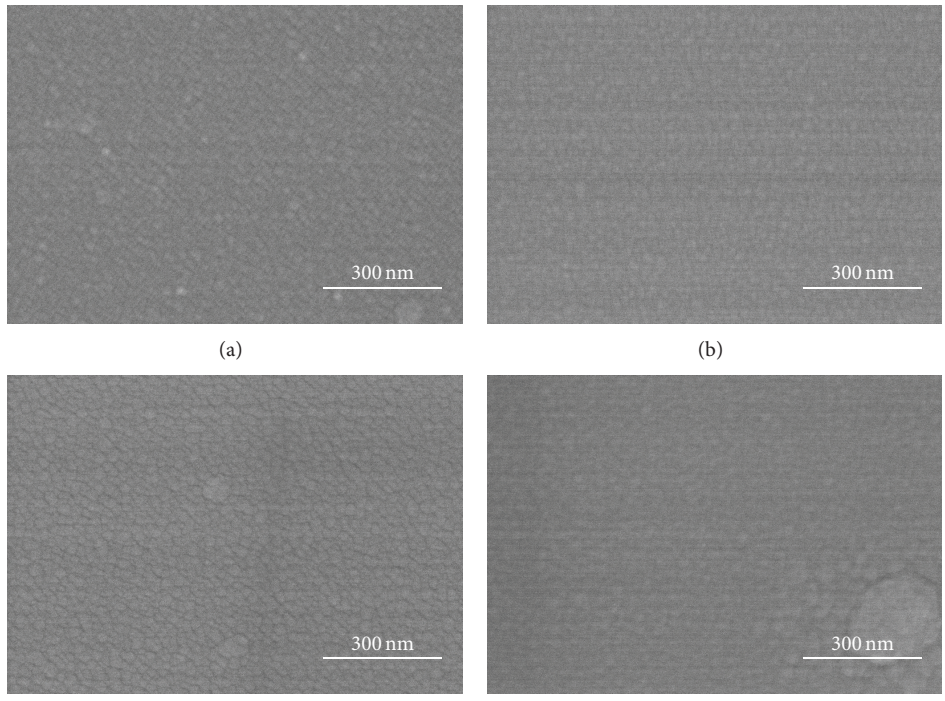

Figure 2: Surface morphology of IGZO thin films as a function of deposition power of In_2O_3 target. (a) 70 W, (b) 80 W, (c) 90 W, and (d) 100 W, respectively.

Ga_2ZnO_4 and spinel rhombohedral $InGaZnO_4$ phases and the phases of precursor In_2O_3, Ga_2O_3, and ZnO were also not observed in Figure 1. One weak and broad peak was assigned to the glass substrate and two weak and broad peaks were assigned to the glass substrate. Those results suggest that all the IGZO thin films exhibit the amorphous phase.

FESEM was used to examine the surface roughness and morphology of the IGZO thin films. Figure 2 shows the FESEM surface images of the IGZO thin films under different deposition powers of In_2O_3 target, which indicates that as deposition power was changed, the surface morphologies had no apparent change as well. As the deposition power of In_2O_3 target was increased from 70 W to 100 W, as Figure 2 shows, morphology of the IGZO thin films exhibited a very smooth surface regardless of deposition power of In_2O_3 target. Surface morphology of all deposited IGZO thin films showed the nanoparticle structure of IGZO grains. Therefore, all IGZO thin films showed stable and flat amorphous surface features. In order to achieve high performance transparent oxide TFTs or memory devices, the preparation of source and drain electrodes with a smooth surface morphology is very important because surface roughness of the IGZO thin films will influence the leakage current between the semiconducting IGZO active layer and source/drain electrodes. The root-mean-square (RMS) surface roughness was measured to be 0.30 nm by AFM, and measured values were 6.357 nm, 7.856 nm, 6.949 nm, and 7.253 nm as the deposition power of In_2O_3 target was 70 W, 80 W, 90 W, and 100 W, respectively. This result suggests that the IGZO thin films deposited by the cosputtering method have the low roughness surfaces and can be used to fabricate the high performance transparent oxide TFTs or memory devices.

Figure 3 shows the cross-section observations of the IGZO thin films as a function of deposition powers of In_2O_3. Calculating the results in Figure 3, thickness of the IGZO thin films increased with increasing deposition powers of In_2O_3 target. Thickness of the IGZO thin films was around 178 nm, 202 nm, 235 nm, and 269 nm, as the deposition powers of In_2O_3 target were 70 W, 80 W, 90 W, and 100 W, respectively. Because the deposition power of GZO target is not changed, the increase in the thickness of the IGZO thin films is caused by the increase of the composition of In_2O_3 in the IGZO thin films. As the crosssection micrographs shown in Figure 3 are compared, there were different results as the deposition power of GZO target was changed. As the deposition power of GZO target was 70 W, the IGZO thin films grew like a densified group of nanowires, which had the structure of highly oriented nanowires parallel to the substrate normal. As 80 W was used as the deposition power of GZO target, the IGZO thin films also grew like a densified group of nanowires, but they had the structure of oriented bars with random direction. As the deposition power of GZO target was 90 W and 100 W, the nanowire-aggregated growths were transformed into the irregular plate-shaped growths with no special direction. These results prove that as the deposition power of GZO target in the cosputtering method is changed, the IGZO thin films have different surface morphology. As we know, ZnO-based thin films have the high *c*-axis orientation in the (00*c*) direction. As lower deposition power of In_2O_3 target is used, ZnO will dominate the growth mechanism

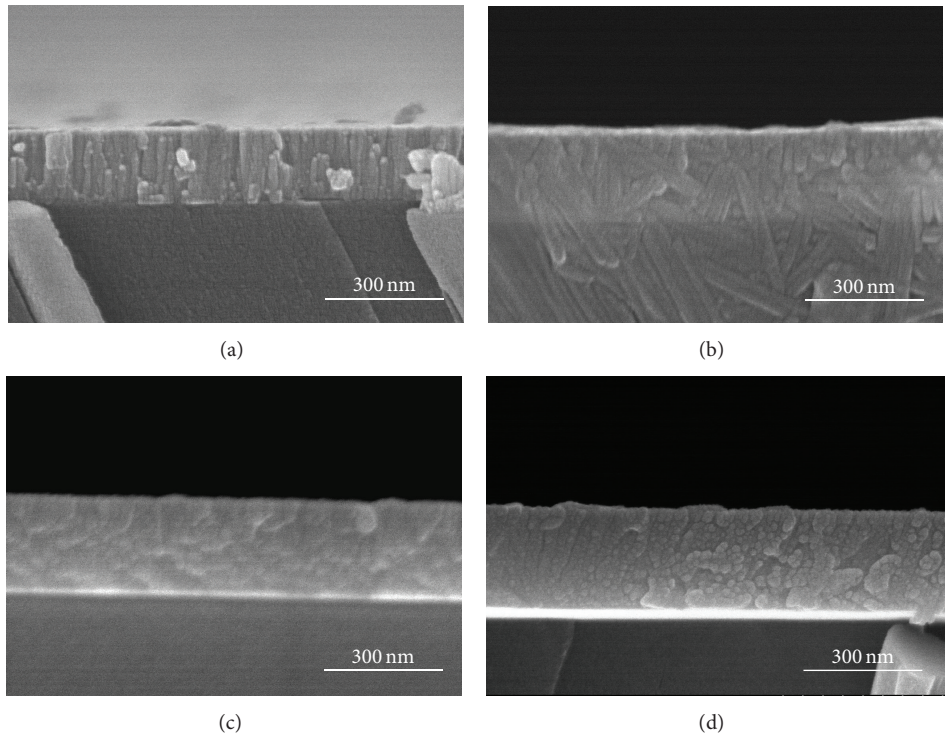

Figure 3: Cross-section observations of IGZO thin films as a function of deposition power of In_2O_3 target. (a) 70 W, (b) 80 W, (c) 90 W, and (d) 100 W, respectively.

and the nanowire-aggregated growths are observed in cross-section of the IGZO thin films. As higher deposition power of In_2O_3 target is used, ZnO cannot dominate and alternating stacks of InO_2^- and $GaO(ZnO)^+$ layers will dominate the growth mechanism. For that, the cross-section of the IGZO thin films shows irregular plate-shaped growths.

In addition, there is no evidence of the segregation of GZO and In_2O_3 due to the uniform cosputtering of GZO and In_2O_3 targets using tilted cathode guns. Nomura et al. reported that IGZO crystal is composed of alternating stacks of InO_2^- and $GaO(ZnO)^+$ layers and the concentration of In_2O_3 has a large effect on the crystallization of IGZO thin films [10]. For the InO_2^- layer an In^{3+} ion is located at an octahedral site coordinated by six oxygens and for the $GaO(ZnO)^+$ layer Ga^{3+} and Zn^{2+} ions are located at trigonal-bipyramidal sites and are each coordinated by five oxygens and alternately stacked along the (0001) direction. As the concentration of In_2O_3 decreases, the crystallization will be inhibited. The results observed from the cross-session images of the IGZO thin films shown in Figure 3 agree with the results of Nomura et al. As Figure 3 shows, as the deposition power of In_2O_3 target is 70 W, the nanowires were parallel to the substrate normal direction. This result suggests the nanowires are stacked along the (0001) direction. As the deposition power of In_2O_3 target increases, the structure of nanowires is changed to irregular plate-shaped growths, which suggests the decrease in the crystallization of the IGZO thin films.

Table 1: Atom ratios of Zn, Ga as a function of deposition power of In_2O_3 target.

In_2O_3 power	Zn	Ga	In
70 W	7.53	10.53	81.94
80 W	5.83	3.86	90.31
90 W	3.56	3.70	92.74
100 W	2.96	3.60	93.44

Due to the large variation in ionization probabilities among different materials, energy dispersive spectrometer (EDS) and secondary ion mass spectrometry (SIMS) are generally considered to be the qualitative techniques. The two methods are used in materials sciences and surface sciences to analyze the composition of solid surfaces and thin films and they can be used to find the variations of atom ratios at the surface (EDS) and at the deposition profile (SIMS) of thin films. Atomic ratio microanalysis in the FESEM is performed by measuring the energy or wavelength and intensity distribution of X-ray signal generated by a focused electron beam on the specimen. With the attachment of EDS, the precise elemental composition of materials can be obtained with high spatial resolution. This suggests that EDS analysis allows one to identify what those particular elements are and their relative proportions, for example, the atomic ratio. Table 1 shows that the atom ratios of Zn and Ga elements decreased and atom ratio of In element

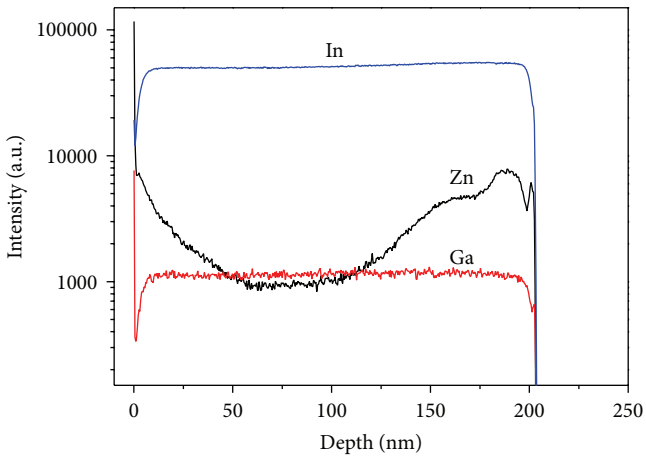

FIGURE 4: Second ion mass spectrometry analysis of IGZO thin film; the deposition power of In_2O_3 target was 100 W.

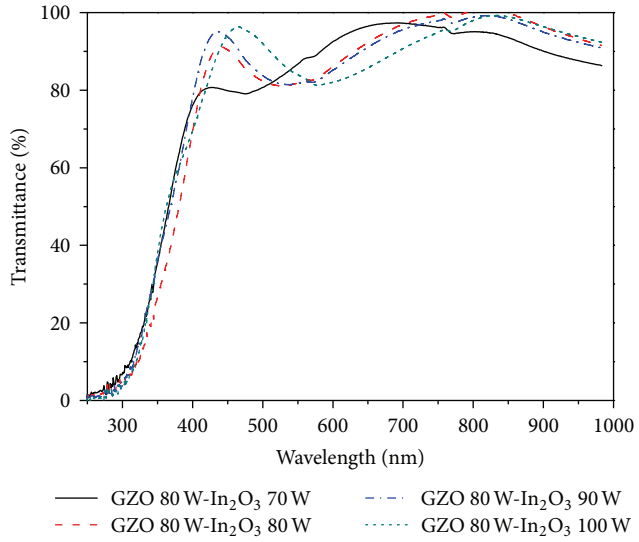

FIGURE 5: Transmittance spectrum of IGZO thin films as a function of deposition power of In_2O_3 target.

increased with increasing deposition power of In_2O_3 target. These results suggest that as the deposition power of In_2O_3 target increases, more atoms will be moved from the surface of In_2O_3 target and then atom ratio of In element increases.

SIMS can analyze the composition by sputtering the surface of specimen with a focused primary ion beam and collecting and analyzing ejected secondary ions. The mass/charge ratios of these secondary ions are measured with a mass spectrometer to determine the elemental, isotopic, or molecular composition of the surface to a depth of 1 to 2 μm. Because SIMS is a high sensitivity surface analysis technique for the determination of surface composition and contaminant analysis and for depth profile in the uppermost surface layers of a sample, it can detect very low concentrations of dopants and impurities. For that, the SIMS analysis was used to find the distribution of Zn, Ga, and In elements in the profile of the IGZO thin films and the results are shown in Figure 4, where the deposition power of In_2O_3 target was 100 W. The IGZO thin films showed that there were incorporations of Zn, Ga, and In atoms in the IGZO thin films, even when the deposition was carried out at room temperature. The concentrations of In and Ga elements in the profile are almost unchanged as the deposition power was increased from 70 W to 100 W. However, the concentration of Zn element in the profile first decreased and then increased as the analyzed depth increased. However, the relative In concentration in the profile of the IGZO thin films is larger than that of the predicted values obtained from the used targets. The variation in Zn concentration is caused by the fact that as GZO target is deposited at 80 W, the decomposition of GZO will happen and the ZnO will vaporize during the deposition process. For that, the Zn concentration is not uniform in the depth profile.

Figure 5 shows the transmission ratios of the IGZO thin films plotted against wavelengths in the region of 250–1000 nm, with deposition time as the parameter. As the deposition power of In_2O_3 target was 70 W, 80 W, 90 W, and 100 W, the average transmittance ratio of the IGZO thin films in the range of 400 nm~700 nm was 87.4%, 86.7%, 87.7%, and 86.6%, and the highest transmittance ratio was 97.4%, 96.9%, 95.6%, and 96.3%, respectively. Those results suggest that as the cosputtering method is used, we can deposit the IGZO thin films with high transmittance ratio. The results in Figure 5 also show that the transmittance ratios in the visible light region are almost unchanged as the deposition power of In_2O_3 target is changed from 70 W to 100 W. However, as the deposition power of In_2O_3 target is changed from 70 W to 100 W, the average transmittance ratios of the IGZO thin films in the range of 400 nm~700 nm have no apparent change. From the results shown in Figure 1, the surfaces of all deposited IGZO thin films reveal a smooth structure and no agglomerated particles are observed, which are the reasons to cause the IGZO thin films having high average transmittance ratios. For the transmission spectra shown in Figure 5, as the different deposition power of In_2O_3 target was used, the shift of the optical band edge was not really observable and a greater sharpness was noticeable in the curves of the absorption edge. Those results suggest that the optical band gap (E_g) values have no apparent change as the cosputtering method is used to prepare the IGZO thin films. Figure 5 also shows that the IGZO thin films deposited on glass substrates had high average transmittance ratios of over 92.7%, 97.6%, 96.3%, and 95.8% in the near-infrared region (700 nm~1000 nm) as the deposition power of In_2O_3 target was 70 W, 80 W, 90 W, and 100 W, respectively.

In the past, determination of the E_g values was often necessary to develop the electronic band structure of a thin-film material. However, as the extrapolation method is used, the E_g values of thin films can be determined from the absorption edge for direct interband transition. The absorption coefficient α was calculated using Lambert's law as follows:

$$\alpha = \ln \frac{(1/T)}{d}, \quad (1)$$

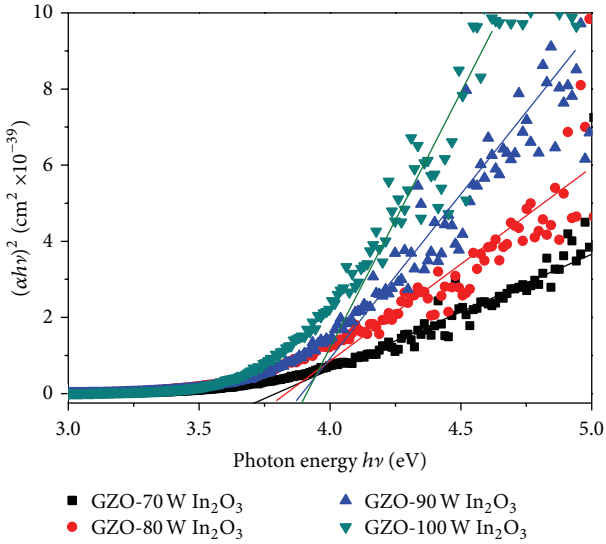

FIGURE 6: $(\alpha h\nu)^2$ versus $h\nu$-E_g plots of IGZO thin films as a function of deposition power of In_2O_3 target.

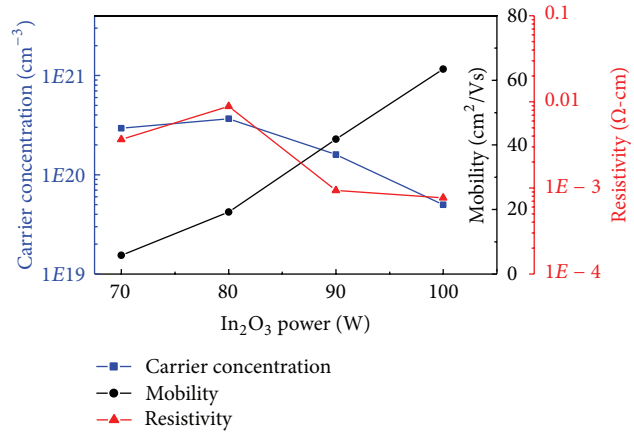

FIGURE 7: Hall mobility, carrier concentration, and resistivity of IGZO thin films as a function of deposition power of In_2O_3 target.

where T and d are thin film's transmittance ratio and thickness. The absorption has a maximum at a high energy and decreases with optical energy in a manner similar to the absorption edge of semiconductors. As the extrapolation method is used, the E_g values of thin films can be determined from the absorption edge, which can be calculated using the relation in (3):

$$(\alpha h\nu)^2 = c\left(h\nu - E_g\right), \tag{2}$$

where α is the optical absorption coefficient, c is the constant for direct transition, h is Planck's constant, and ν is the frequency of the incident photon [14]. The linear dependence of $(\alpha h\nu)^2$ on $h\nu$ indicates that the IGZO thin films are direct transition type semiconductors. In accordance with (3), as Figure 6 shows, the calculated E_g values of the IGZO thin films increased from 3.71 eV, 3.79 eV, and 3.84 eV to 3.87 eV as the deposition power of In_2O_3 target was increased from 70 W, 80 W, and 90 W to 100 W, respectively. Because ZnO, Ga_2O_3, and In_2O_3 thin films have different E_g values, the variation in E_g values is believed to be caused by the variation in the composition of the IGZO thin films.

When the IGZO thin films are deposited using the cosputtering method, three reasons are believed to influence the carrier mobility of IGZO thin films. First, depositing at room temperature cannot provide enough energy to enhance the motion of plasma molecules, which will improve the crystallization and grain size growth of IGZO thin films, and the defects in the IGZO thin films will be generated during the deposition process. Second, if the agglomerated particles in the IGZO thin films increase, that will cause the decrease in the inhibiting of the barriers electron transportation and the mobility will increase. Third, Hosono showed that, from the electron mobility and concentrations evaluated from the Hall effects for amorphous IGZO thin films with different compositions, the mobility is primarily determined by the fraction of In_2O_3 content and the highest value of ~40 cm^2 (V s)$^{-1}$ is obtained around the samples containing the maximum In_2O_3 fraction [15]. From those reasons, the carrier mobility, carrier concentration, and resistivity of the IGZO thin films are believed to be dependent on deposition power (or concentration) of In_2O_3.

However, as Figure 7 indicates the electrical properties of the IGZO thin films, the carrier concentration linearly decreased as the deposition power of In_2O_3 target was larger than 80 W and the carrier concentration decreased from 3.67 × 10^{20} cm^{-3} to 4.98 × 10^{19} cm^{-3}, respectively. The carrier mobility linearly increased from 5.83 cm^2/V-s to 63.5 cm^2/V-s as the deposition power of In_2O_3 target increased from 70 W to 100 W. Those results suggest that the concentration of In_2O_3 is the most important factor to influence the mobility of the IGZO thin films and the results agree with the important results investigated by Hosono [15]. The resistivity of TCO thin films is proportional to the reciprocal of the product of carrier concentration N and mobility μ:

$$\rho = \frac{1}{Ne\mu}. \tag{3}$$

Both the carrier concentration and the carrier mobility contribute to the conductivity. As the deposition power of In_2O_3 target was changed from 70 W to 100 W, the resistivity of the IGZO thin films was changed from 8.85 × 10^{-3} Ω-cm to 7.68 × 10^{-4} Ω-cm. The minimum resistivity of the IGZO thin films at a deposition power of In_2O_3 target of 100 W is mainly caused by the carrier mobility at its maximum.

4. Conclusions

The characteristics of the IGZO thin films prepared by Ga_2O_3-2 ZnO (GZO) cosputtered In_2O_3 method were well investigated in this study. As deposition time was 30 min, thickness of the IGZO thin films was around 178 nm, 202 nm, 235 nm, and 269 nm, as the deposition powers of In_2O_3 target were 70 W, 80 W, 90 W, and 100 W, respectively. As the deposition power of In_2O_3 target was 70 W, 80 W, 90 W, and 100 W, the average transmittance ratio of the IGZO thin films

in the range of 400 nm~700 nm was 87.4%, 86.7%, 87.7%, and 86.6%, and the calculated E_g values increased from 3.72 eV, 3.79 eV, and 3.84 eV to 3.87 eV, respectively. As the deposition power of In_2O_3 target increased from 70 W to 100 W, the carrier mobility of IGZO thin films linearly increased from 5.83 cm^2/V-s to 63.5 cm^2/V-s. The mobility of 63.5 cm^2/V-s is higher than that of most reported IGZO thin films. We had found that the IGZO thin films deposited by the cosputtering method had the low roughness surfaces and could be used to fabricate the high performance transparent oxide TFTs or memory devices.

Conflict of Interests

The authors declare that there is no conflict of interests regarding the publication of this paper.

Acknowledgment

The authors acknowledge financial support of NSC 102-2221-E-218-036, NSC 102–2622-E-390-002-CC3, and NSC 102-2221-E-390-027.

References

[1] J. Kanicki, F. R. Libsch, J. Griffith, and R. Polastre, "Performance of thin hydrogenated amorphous silicon thin-film transistors," *Journal of Applied Physics*, vol. 69, no. 4, pp. 2339–2345, 1991.

[2] T. C. Fung, *Amorphous In-Ga-Zn-O thin film transistor for future optoelectronics [Ph.D. thesis]*, University of Michigan, Ann Arbor, Mich, USA, 2010.

[3] J.-H. Lan and J. Kanicki, "Planarized copper gate hydrogenated amorphous-silicon thin-film transistors for AM-LCDs," *IEEE Electron Device Letters*, vol. 20, no. 3, pp. 129–131, 1999.

[4] J.-H. Lan and J. Kanicki, "Buried busline a-Si:H TFT structures for AM-LCDs," in *Proceedings of the Active-Matrix Liquid Crystal Displays (AM-LCD '98)*, pp. 77–81, 1998.

[5] J. H. Song, H. L. Ning, W. G. Lee, S. Y. Kim, and S. S. Kim, "Views on the low-resistant bus materials and their process architecture for the large-sized post-ultra definition TFT-LCD," in *Digest Technique Papers IMID 2008*, vol. 8, pp. 9–12, 2008.

[6] T. Urabe, "The outstanding potential of OLED displays for TV applications," *Information Display*, vol. 24, no. 9, pp. 14–17, 2008.

[7] K. Nomura, H. Ohta, K. Ueda, T. Kamiya, M. Hirano, and H. Hosono, "Thin-film transistor fabricated in single-crystalline transparent oxide semiconductor," *Science*, vol. 300, no. 5623, pp. 1269–1272, 2003.

[8] K. Nomura, H. Ohta, A. Takagi, T. Kamiya, M. Hirano, and H. Hosono, "Room-temperature fabrication of transparent flexible thin-film transistors using amorphous oxide semiconductors," *Nature*, vol. 432, no. 250, pp. 488–492, 2004.

[9] H. Ohta, K. Nomura, M. Orita et al., "Single-crystalline films of the homologous series $InGaO_3(ZnO)_m$ grown by reactive solid-phase epitaxy," *Advanced Functional Materials*, vol. 13, no. 2, pp. 139–144, 2003.

[10] K. Nomura, T. Kamiya, H. Ohta, T. Uruga, M. Hirano, and H. Hosono, "Local coordination structure and electronic structure of the large electron mobility amorphous oxide semiconductor In-Ga-Zn-O: experiment and ab initio calculations," *Physical Review B*, vol. 75, no. 3, Article ID 035212, 2007.

[11] C. Lo and T. Hsieh, "Preparation of IGZO sputtering target and its applications to thin-film transistor devices," *Ceramics International*, vol. 38, no. 5, pp. 3977–3983, 2012.

[12] J. A. Jeong and H. K. Kim, "Transparent Ga and Zn co-doped In_2O_3 electrode prepared by co-sputtering of Ga:In_2O_3 and Zn:In_2O_3 targets at room temperature," *Thin Solid Films*, vol. 519, no. 10, pp. 3276–3282, 2011.

[13] Y. S. Jung, K. H. Lee, W.-J. Kim, W.-J. Lee, H.-W. Choi, and K. H. Kim, "Properties of In-Ga-Zn-O thin films for thin film transistor channel layer prepared by facing targets sputtering method," *Ceramics International*, vol. 38, supplement 1, pp. S601–S604, 2012.

[14] F. H. Wang, C. F. Yang, and M. C. Liu, "Using flexible polyimide as a substrate to deposit ZnO:Ga thin films and fabricate p-i-nα-Si:H thin-film solar cells," *International Journal of Photoenergy*, vol. 2013, Article ID 263213, 7 pages, 2013.

[15] H. Hosono, "Ionic amorphous oxide semiconductors: material design, carrier transport, and device application," *Journal of Non-Crystalline Solids*, vol. 352, no. 9–20, pp. 851–858, 2006.